

## An Enzymatically Synthesized Polyaniline: A Solid-State NMR Study

Sangrama K. Sahoo,<sup>†</sup> Ramaswamy Nagarajan,<sup>†</sup> Sucharita Roy,<sup>†</sup>  
Lynne A. Samuelson,<sup>‡</sup> Jayant Kumar,<sup>†</sup> and Ashok L. Cholli<sup>\*,†</sup>

Center for Advanced Materials, University of Massachusetts Lowell, Lowell, Massachusetts 01854,  
and Natick Soldier Center, U.S. Army Soldier and Biological Chemical Command,  
Natick, Massachusetts 01760

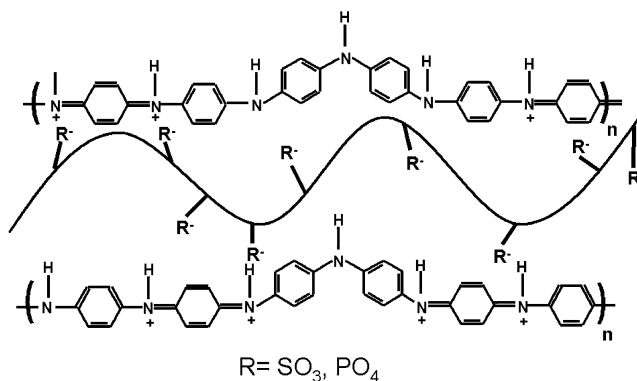
Received August 23, 2003; Revised Manuscript Received March 16, 2004

**ABSTRACT:** The variation in molecular and electronic structure of doped (as synthesized) conducting, dedoped base, and redoped conducting forms of polyaniline (PANI) prepared by oxidative enzymatic polymerization of aniline with and without the presence of polyelectrolyte template was analyzed by solid-state <sup>13</sup>C and <sup>15</sup>N CP/MAS NMR spectroscopy. Polyanilines were enzymatically synthesized using a natural biocatalyst such as horseradish peroxidase (HRP) at pH 4.3 and a synthetic biomimetic catalyst, specifically poly(ethylene glycol)-coupled hematin (PEG-hematin), at pH 1.0. The HRP-catalyzed enzymatic polymerization of PANI was carried out in the presence of macromolecular polyelectrolyte templates such as poly(vinylphosphonic acid) (PVP), poly(4-styrenesulfonate) (SPS), and dodecylbenzenesulfonic acid (DBSA). <sup>13</sup>C and <sup>15</sup>N CP/MAS NMR spectral features indicate that the PANI obtained by PEG-hematin-catalyzed enzymatic polymerization resembles most with chemically synthesized analogues in its doped (as synthesized) conducting form than other forms of PANI. A systematic experiment involving a redoping process at different pH levels shows the structural changes during the transformation from dedoped base form to redoped conducting form. Solid-state NMR data also indicate a decrease of polaronic contribution at the higher doping level. End-group analysis from <sup>15</sup>N CP/MAS NMR data provides information on the molecular weight of the enzymatically polymerized PANI sample.

## Introduction

In recent years, the molecular and electronic structure of intrinsically conducting polyaniline (PANI) has attracted considerable interest because of its extensive use in a wide variety of optoelectronic applications.<sup>1,2</sup> The most probable conducting form of PANI is the emeraldine salt form, normally produced by an oxidative polymerization of aniline in aqueous acids.<sup>3,4</sup> It is an electrically conducting polymer ( $\sigma \sim 10^{-2}$ – $10^3$  S cm<sup>-1</sup>) due to the presence of cation radicals (polarons) on the nitrogen of its backbone structure. The positive charge on the PANI backbone is normally neutralized by negatively charged counterions, typically, sulfate, chloride, or phosphate anions. In a doped PANI sample, the charge transport properties are mostly determined by the molecular interactions among polymer chains, dopant, and solvent medium.<sup>5</sup> The polymer chain conformation (interpolymer packing) and the charge distribution along the polymer backbone are of significant interest to optimize the conductivity as well as the processability of polyaniline.<sup>2,6,7</sup> This warrants a better understanding of polyaniline structures that varies significantly with synthesis procedures and postsynthesis treatments. Until recently, the structural characterization was focused mainly on the chemically and electrochemically synthesized PANI in both the conducting and insulating form. Recent efforts have resulted in the development of a unique enzymatic approach (horseradish peroxidase (HRP) as catalyst and H<sub>2</sub>O<sub>2</sub> as an oxidizing agent) for the polymerization of aniline in the presence of a polyelectrolyte template such as poly(4-styrenesulfonate) (SPS) or poly(vinylphosphonic acid) (PVP) under mild aqueous pH 4.3 buffer conditions (Scheme 1).<sup>8–11</sup> This process promotes para-directed, head-to-tail polymeri-

**Scheme 1. Complex Formation of Macromolecular Polyelectrolyte Template along with Polyaniline Chain**



zation of aniline by preferentially aligning them onto a polyanionic template and thus making the doped (as synthesized) PANI water-soluble. It appears that this process inherently minimizes the parasitic branching. The solid-state <sup>13</sup>C and <sup>15</sup>N CP/MAS NMR data along with spectroscopic data from UV–vis and FTIR show that the structural features of dedoped (base) form of the enzymatically synthesized PANI–PVP complex is in the emeraldine base form and resembles with the chemically synthesized PANI.<sup>11,12</sup> Peroxidase enzyme also polymerizes aniline in micelles of SDBS (sodium dodecylbenzenesulfonic acid) solution to provide highly conducting and soluble polyaniline in which SDBS acts as a template.<sup>13</sup> However, enzymatic polymerization using HRP as enzyme in the absence of an anionic template yields mostly a branched PANI.<sup>14</sup>

Recently, a novel modified enzyme hematin (hydroxy-ferritroporphyrin) with tethered poly(ethylene glycol) (PEG) chains as a flexible and hydrophilic linker (PEG-hematin) has been developed for its use as a biocatalyst

<sup>†</sup> University of Massachusetts Lowell.

<sup>‡</sup> U.S. Army Soldier and Biological Chemical Command.

in the enzymatic polymerization.<sup>15,16</sup> This novel synthetic enzyme is an inexpensive alternative to the use of HRP for the synthesis of polyaniline and polyphenols. The absence of amino acid residues in the synthetic enzyme significantly improves its stability in a wider range of pH conditions. The novelty in this approach of biomimetic polymerization of aniline at very low pH is that the polyaniline is water-soluble and highly conducting without the use of macromolecular polyelectrolyte templates.<sup>17</sup> It is believed that the low-pH environment is responsible for the linear chain growth of polyaniline.<sup>10</sup> However, it is imperative to know the structure of various forms of polyaniline as well as charge dynamics in the doped state to understand the role of synthetic conditions (presence and absence of polyelectrolyte template during enzymatic polymerization) and postsynthesis treatments (effect of redoping) on its molecular structure and conducting properties.

In this respect, modern high-resolution solid-state NMR techniques offer a promising way to analyze the structural and conformational properties of these materials. Conventionally solid-state <sup>13</sup>C and <sup>15</sup>N NMR spectroscopy have been used for the structural characterization of various forms of PANI.<sup>18–22</sup> Preliminary research by MacDiarmid et al. focused on the characterization of doped and dedoped form of chemically synthesized PANI by solid-state <sup>13</sup>C and <sup>15</sup>N CP/MAS NMR<sup>19,23,24</sup> and showed that the broad <sup>13</sup>C line widths for the PANI in the emeraldine hydrochloride state are inhomogeneously broadened, and the chemical shifts dispersion reflects a structural disorder resulting from the disruptions in electron delocalization. In addition, <sup>15</sup>N CP/MAS NMR data suggested the existence of an alternating benzenoid and quinoid repeating units in the emeraldine base form of PANI.<sup>24</sup> This pioneering work followed by quite a number of studies dealing with different aspects of conducting PANI that have been reported in the following years showed the intricacies involved in its structure and the charge distribution.<sup>12,20–22,25–28</sup> The presence of unpaired electrons in the ordered crystalline regions (pseudo-metallic and conducting regions) were studied by Espe et al.,<sup>21</sup> and it was demonstrated by <sup>15</sup>N–<sup>19</sup>F REDOR experiments that amorphous regions of the PANI chains are arranged with an in-plane interchain separation of 10 Å. Furthermore, solid-state NMR studies by Kababya et al. on the electrochemically synthesized PANI–DBSA system revealed the variation in the structure and properties of their synthesized material from chemically synthesized PANI.<sup>22</sup> On the other hand, our studies on the enzymatically synthesized PANI–PVP complex by solid-state <sup>13</sup>C and <sup>15</sup>N CP/MAS NMR revealed that the structure of PANI in dedoped base form is quite similar to chemically synthesized samples.<sup>12</sup> It is demonstrated that it is possible to completely remove the template from the enzymatically synthesized PANI–PVP complex after its role in promoting linear chain growth. However, as stated above, considering the fact that PANI obtained by different methods shows different structures and properties, it is interesting to study and compare various forms of PANI synthesized by enzyme and biomimetic catalyst as well as dopants, which plays a significant role in the processability and electrical conductivity.

In the present work, both the <sup>13</sup>C and <sup>15</sup>N solid-state CP/MAS NMR spectroscopic techniques were used as a tool for structural elucidation of PANI and PANI–polyelectrolyte complex synthesized by different en-

zymes and compared the effect of enzymatic synthetic conditions on the charge distribution and structural heterogeneity. Two different catalysts (HRP and PEG-hematin) were used for the synthesis of PANI. The PANI synthesized by PEG-hematin-catalyzed enzymatic polymerization is reported as PANI–H. In the case of HRP-catalyzed enzymatic polymerization, three different polyelectrolyte templates were used for the synthesis of PANI–polyelectrolyte complex and henceforth mentioned as PANI–PVP, PANI–SPS, and PANI–DBSA complex for PVP, SPS, and DBSA templates, respectively. The dedoping of as-synthesized conducting PANI–PVP complex resulted in the complete removal of PVP; henceforth, the dedoped and redoped form of this sample is labeled as PANI–P.

## Experimental Section

**Materials and Sample Preparation.** Horseradish peroxidase (HRP, EC 1.11.1.7) type II, 150–200 units/(mg of solid), and hematin were purchased from Sigma Chemical Co., St. Louis, MO. Aniline monomer (purity 99.5%), hydrogen peroxide (30%), and poly(sodium 4-styrenesulfonate) (SPS), 100 kDa, sodium salt were purchased from Aldrich Chemical Inc., Milwaukee, WI, and used as received. Poly(vinylphosphonic acid), 24 kDa, was obtained from Polysciences Inc. and used as received. <sup>15</sup>N-labeled aniline (99%) was obtained from Cambridge Isotope Inc., Andover, MA.

**Synthesis of PANI–Polyelectrolyte Complex.** *HRP-Catalyzed Synthesis:* The polymerization of aniline in the presence of various polyelectrolyte templates (PVP, SPS, and DBSA) was performed in 200 mL of 10 mM sodium phosphate buffer at a pH of 4.3. In a typical polymerization reaction, equimolar quantities (typically 10 mM) of the polyelectrolyte template (molarity estimated on the basis of molecular weight of repeat unit) and aniline (regular/<sup>15</sup>N-labeled) were dissolved in the phosphate buffer at 25 °C, and the pH was adjusted to 4.3. To this solution, 2 mL of HRP stock solution (10 mg in 1 mL of deionized water) was added with constant stirring. Finally, an equimolar amount (typically 10 mM) of diluted hydrogen peroxide solution (3% solution in deionized water) was added in small aliquots over a period of 1 h with constant stirring. The reaction mixture was stirred for 4 h to complete the polymerization. In the case of the PANI–PVP complex, the green precipitate was filtered through 1 μm nucleopore track-etch membrane and washed repeatedly with acidified 1:1 acetone/deionized water solution for the removal of unreacted aniline monomer and enzyme. The precipitate was dried in a vacuum oven at 60 °C for 48 h and used for further characterization. The gravimetric yield was around 78%. In the case of PANI–DBSA and PANI–SPS complexes, final mixtures were transferred to individual regenerated natural cellulose membrane bags (molecular weight cutoff 1000 Da) and were dialyzed against a large excess (5000 mL) of acidified deionized water maintained at pH 4.0. The dialysis process was carried out for 72 h with fresh acidified DI water solution used every 12 h to expedite the removal of oligomers and unreacted monomer. These solutions were evaporated to obtain the green precipitate. The PANI–polyelectrolyte complex was dried in a vacuum oven at 60 °C for 48 h.

*PEG-Hematin-Catalyzed Synthesis of Self-Doped PANI:* The PEG-hematin polymerization of aniline (regular/<sup>15</sup>N-labeled) was carried out at 25 °C in 100 mM sodium phosphate buffer at pH 1.0. In a typical reaction, 2.5 mL of aniline and 5 mL of PEG-hematin stock solution (0.65 mg/mL) were added to 500 mL of phosphate buffer with constant stirring. To this solution, 500 μL of hydrogen peroxide (30% solution) was added with constant stirring. The reactants were stirred for 12 h to complete the polymerization followed by precipitation of the PANI complex. The precipitate obtained was thoroughly washed with acidified acetone to remove unreacted monomer and any oligomeric products. The final purified PANI was dried in the vacuum oven at 60 °C for 48 h.

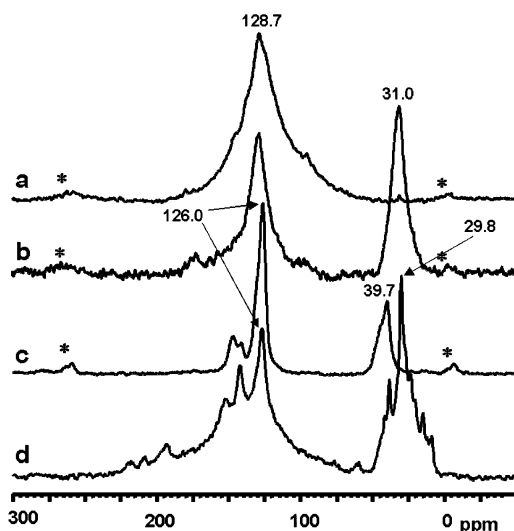


**Figure 1.**  $^{13}\text{C}$  CP/MAS NMR spectra of enzymatically synthesized PANI in its self-doped as-synthesized conducting form: (a) PANI-H; (b) PANI-PVP complex; (c) PANI-SPS complex; (d) PANI-DBSA complex (\* denotes spinning sideband).

Conductivity measurements were carried out using a Cascade Microtech four-point probe connected to a current source and electrometer on as-synthesized conducting, dedoped base, and redoped conducting forms of PANI samples that were pressed into pellets. The conductivity values reported are the average of 5–6 readings at different surface sites and side regions of the disk.

**Solid-State NMR Measurements.** Solid-state  $^{13}\text{C}$  and  $^{15}\text{N}$  NMR experiments were carried out on a Bruker DMX 7.05 T wide bore magnet system equipped with a 4 mm triple resonance broadband probe. Zirconium oxide ( $\text{ZrO}_2$ ) (4 mm o.d.) rotors were used with Kel-F caps for all the measurements. The NMR measurements were carried out at room temperature unless otherwise stated. Cross-polarization with magic angle spinning (CP/MAS) and dipolar decoupling (DD) techniques were used to study these materials. A one-time magic angle adjustment was accomplished by maximizing the spinning sideband intensities of  $^{79}\text{Br}$  NMR signal of KBr sample. Glycine was used to setup Hartmann–Hahn matching condition using a ramped cross-polarization method. All spectra were recorded using a rotor spinning speed of 10.0 kHz (except a few of  $^{13}\text{C}$  and  $^{15}\text{N}$  CP/MAS NMR experiments were done with 5 kHz spinning speed, and these are mentioned in the text). The typical parameters for  $^{13}\text{C}$  CP/MAS NMR experiments were as follows: spin-lock field of 70.0 kHz, a 35.0 ms acquisition time, a 3.0 s recycle time, contact time of 1.0–2.0 ms, and a sweep width of 31.0 kHz. The total number of free induction decays (FIDs) co-added per spectrum ranged from 10 000 to 20 000. All the FIDs were processed by an exponential and in some instances a Gaussian apodization function with a 30.0–40.0 Hz line broadening. All the  $^{13}\text{C}$  CP/MAS NMR spectra were externally referenced to glycine by assigning the carbonyl signal at 176.03 ppm with respect to tetramethylsilane (TMS) resonance at 0.0 ppm. For  $^{15}\text{N}$  CP/MAS NMR, a  $\pi/2$  pulse width of 4.8  $\mu\text{s}$ , a recycle time 4.0 s, a contact time of 3.0–5.0 ms, and a sweep width of 31.0 kHz were used along with 15 000–40 000 FIDs, which were co-added to get reasonable signal-to-noise ratio. The spectra were externally referenced to the  $^{15}\text{N}$  signal of solid ammonium sulfate at 0.0 ppm.

## Results and Discussion

**$^{13}\text{C}$  Measurements.** The solid-state  $^{13}\text{C}$  CP/MAS NMR spectra of the doped conducting form of PANI-H, PANI-PVP, PANI-SPS, and PANI-DBSA complex are shown in parts a–d of Figure 1, respectively. In Figure 1a, a featureless broad resonance centered at

$\sim 128.7$  ppm appears and spread over the 200.0 ppm region of the  $^{13}\text{C}$  CP/MAS NMR spectrum. Spinning sidebands (marked as “\*”) appear on both side of the isotropic signal. The  $^{13}\text{C}$  CP/MAS NMR spectral feature for this sample is entirely due to the aromatic ring carbons of the polyaniline backbone. The absence of any noticeable resonances (from PEG) in the aliphatic region of the spectrum indicates the complete removal of the enzyme during the postsynthesis washing. The spectral features (single broad line) resemble well with the chemically synthesized PANI doped with either hydrochloric acid or camphorsulfonic acid.<sup>19,29</sup> However, the line width for PANI is only 40 ppm compared to the nearly 60 ppm line width observed for chemically synthesized analogues. The lower line width also reflects a lower conductivity value of enzymatically synthesized PANI.

The PANI obtained by template-assisted enzymatic polymerization of aniline using HRP as a catalyst shows two sets of resonances in each spectrum (Figure 1b–d). The  $^{13}\text{C}$  CP/MAS NMR of the PANI-PVP complex shows a broad resonance at  $\sim 128.6$  ppm, corresponding to polyaniline backbone.<sup>12</sup> However, the broadening of this resonance peak (line width  $\sim 20$  ppm) is lower compared to the spectrum in Figure 1a, and it spreads over 125.0 ppm of the  $^{13}\text{C}$  chemical shift region. Furthermore, a comparatively a narrow resonance peak appears at 31.0 ppm due to the aliphatic ( $-\text{CH}$  and  $-\text{CH}_2$ ) carbons of the PVP polyelectrolyte template.<sup>12</sup> As there are no overlapping resonances from the template on the resonances of PANI backbone in the  $^{13}\text{C}$  CP/MAS NMR spectrum (Figure 1b), this proved to be an ideal system for the study of spectral features of PANI in the presence of a macromolecular polyelectrolyte template.<sup>14</sup> In contrast, although the PANI synthesized by a template-assisted enzymatic polymerization in the presence of SPS yields a similar complex (green precipitate and strong UV–vis–near-IR polaron band near 823 nm),<sup>10</sup> there is no indication of a broad spectral pattern in aromatic region ( $\sim 128.0$  ppm) in the  $^{13}\text{C}$  CP/MAS NMR spectrum. In fact, peaks at 126.0, 140.9, and 147.0 ppm in the aromatic region and a 39.7 ppm peak along with a shoulder resonance at 44.0 ppm in the aliphatic region are observed due to the SPS polyelectrolyte template. The assignments of these resonances are confirmed by comparing the chemical shifts of the SPS sample. Although the difference spectrum was obtained considering the ratio of PANI and SPS subunits in the conducting complex, it fails to provide additional information about the PANI resonances in the spectrum. However, the doped conducting form of PANI obtained by enzymatic polymerization of aniline and DBSA micellar template shows a broad hump in the aromatic region of the  $^{13}\text{C}$  CP/MAS NMR spectrum overlapped with resonances at 126.0, 141.4, and 152.4 ppm. The broad resonance for this sample extends from 0.0 ppm to over 250.0 ppm. These features are similar to the one reported for the PANI-DBSA complex obtained by electrochemical oxidation of aniline.<sup>22</sup> Several narrow resonances due to the long aliphatic chains of the DBSA template appear in the 10.0–50.0 ppm region. This spectrum was recorded with a magic angle spinning speed of 5 kHz; the sidebands now appear at  $\sim 70.0$  and 200.0 ppm. The spectral features of these four PANI samples are different and may be due to the variation in molecular structures as well as extent of dopant interaction with the PANI backbone. This varia-

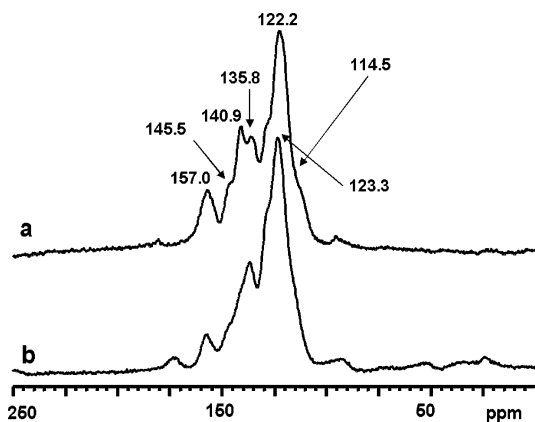


**Figure 2.**  $^{13}\text{C}$  CP/MAS NMR spectra of enzymatically synthesized PANI in its dedoped base form: (a) PANI-H; (b) PANI-P.

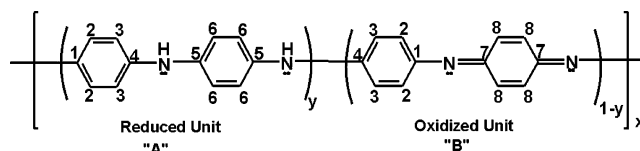
tion was also reflected in their conductivity measurements.

The conductivity of these samples varied depending on the nature of the enzymatic polymerization as well as the type of template used in the synthesis. The doped conducting form of PANI-H shows conductivity ( $\sigma$ ) on the order of  $\sim 10^{-1}$  S/cm. In contrast, PANI-PVP and PANI-SPS complexes exhibit conductivity on the order of  $\sim 10^{-2}$  S/cm. The highest conductivity is observed in the case of the PANI-DBSA complex and is on the order of  $\sim 10$  S/cm. This variation in the conductivity values is related to their  $^{13}\text{C}$  CP/MAS NMR spectral features. It is interesting to note that as the conductivity increases, the line widths of the aromatic resonance increase. The PANI-DBSA complex exhibiting the highest conductivity shows the largest line width ( $\sim 60.0$  ppm), while the line width is  $\sim 20.0$  ppm for the PANI-PVP complex, for which the conductivity is 3 orders of magnitude less. PANI obtained from the PEG-hematin-catalyzed enzymatic polymerization without any macromolecular template shows an intermediate conductivity as well as line width ( $\sim 40.0$  ppm).

Figure 2a,b shows the  $^{13}\text{C}$  CP/MAS NMR spectra of the dedoped (base) form of PANI-H and PANI-P. The  $^{13}\text{C}$  CP/MAS NMR spectrum of PANI-H shows considerable line narrowing upon dedoping when compared to the parent-doped (conducting) form. The resonances in the aromatic region of the spectrum spread over a narrow range of 80.0 ppm, displaying many resolved peaks. The assignment of these resonances to the emeraldine base form of PANI agrees well with the previous reported chemically and electrochemically synthesized PANI data.<sup>19,22</sup>

The strong resonance peak at 122.2 ppm is assigned to protonated carbons of the benzenoid ring directly attached to the quinoid ring (C2, C3), and quinoid protonated ring carbons appear at 135.8 ppm (C8). Protonated carbons of the benzenoid rings that are one ring away from quinoid rings appear at 114.5 ppm (C6). Other nonprotonated carbons corresponding to both benzenoid and quinoid rings appear below 140.0 ppm and are marked in Figure 2a. However, the chemical shift of the protonated benzenoid ring carbons (C2, C3) appears 1.0 ppm upfield than reported earlier by Kaplan et al.,<sup>19</sup> while other chemical shifts are well within the error limit of peak picking software. Another interesting observation is the presence of a distinct shoulder at 128.4 ppm in dedoped base form and was not reported in the chemically synthesized dedoped PANI. This is an

indication of the presence of residual conducting regions even after dedoping and concur with the observation of partial dedoping of doped PANI in  $\text{NH}_4\text{OH}$  solution by Kababya et al.<sup>22</sup> Figure 2b shows the  $^{13}\text{C}$  CP/MAS NMR spectrum of the PANI-PVP complex in its dedoped base form (PANI-P).<sup>12,14</sup> In the case of dedoped PANI-P, one point worth repeating here from our earlier work is that the observation of the complete removal of polyelectrolyte template (PVP) from the PANI-PVP complex during the dedoping process. The novelty of using this template method is that it can be removed after directing the linear PANI chain growth. However, comparing the two spectra in Figure 2 shows that the resonance peaks for carbons (C5 and C6) corresponding to benzenoid rings, which are one ring away from quinoid rings, are not well resolved. Two resonances at 135.8 (C8) and 140.9 ppm are well-separated in Figure 2a while only one resonance is observed at 136.4 ppm in Figure 2b. A weak shoulder appears at 141.3 ppm in Figure 2b. The resonance at 157.0 ppm assigned to nonprotonated quinoid carbons (C8) is less intense in spectrum b compared spectrum a in Figure 2. This suggests that there are considerable structural variations in these two PANI samples, although the overall spectral pattern looks similar. One possible difference may be in the distribution of reduced and oxidized units. Because of lack of spectral resolution in the  $^{13}\text{C}$  NMR spectrum, it is not possible to unambiguously quantify the fraction of reduced and oxidized units. However, on the other hand,  $^{15}\text{N}$  NMR provides detailed structural variations of PANI simply because of its wide chemical shift dispersion. It may be helpful to compare both the  $^{13}\text{C}$  and  $^{15}\text{N}$  NMR spectra of dedoped PANI for understanding of the structural variations. The significance of the solid-state  $^{15}\text{N}$  NMR application to PANI is also discussed in this section.



Parts a and b of Figure 3 show the  $^{13}\text{C}$  CP/MAS NMR spectra of the redoped conducting form of PANI-H and PANI-P, respectively. The redoping of the dedoped base form of PANI-H is carried out in the HCl medium at a similar pH environment as of parent-doped synthesis. The conductivity ( $\sigma$ ) of the redoped PANI-H and PANI-P is nearly same as of the parent-doped form. Figure 3a is less broadened compared to its parent-doped spectrum (as synthesized) (Figure 1a) (reduction in line width by 4.0 ppm), while it is reverse for PANI-P in its redoped form (increase in line width by 10.0 ppm). The increase of  $^{13}\text{C}$  line width from 20.0 to 30.0 ppm in redoped PANI-P despite not so obvious change in its conductivity (conductivity remains same in as-synthesized and redoped PANI) indicates that the change in the morphology due to rearrangements of polymer chains after removal of the macromolecular polyelectrolyte template. The removal of the macromolecular template may provide better interaction among PANI chains, thus causing line broadening due to heterogeneity in its structure. Note that although the line width increases due to increase heterogeneity, it is not enough to increase the conductivity of PANI as the heterogeneity is still low compared to other PANI samples (may

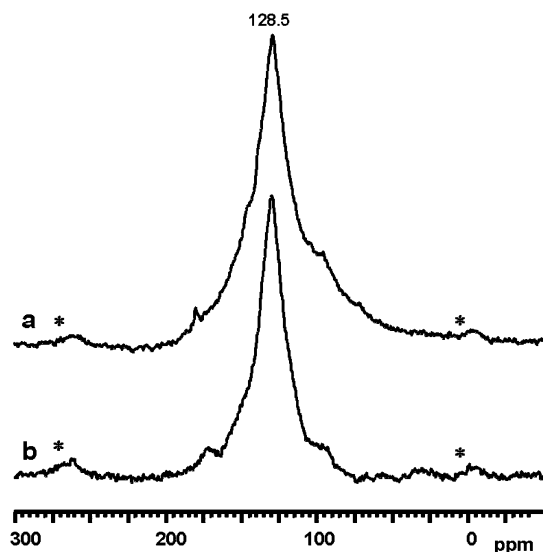


**Figure 3.**  $^{13}\text{C}$  CP/MAS NMR spectra of enzymatically synthesized PANI in its redoped conducting form: (a) PANI-H; (b) PANI-P (redoping was carried out in HCl medium) (\* denotes spinning sideband).

be due to the low molecular weight of the polymer). However, the PANI-H have the same dopant, i.e., chloride ion in its doped (as synthesized) and redoped form and thus no change in either  $^{13}\text{C}$  line width or conductivity between two forms.

The  $^{13}\text{C}$  CP/MAS NMR spectral pattern of doped (as synthesized), dedoped, and redoped form of PANI-H indicates that it is possible to synthesize highly conducting linear PANI without the use of macromolecular polyelectrolyte templates. A low-pH medium is necessary for the synthesis of conducting PANI by biomimetic catalysis. The natural enzyme will be denatured when the pH of the enzyme solution reaches pH 3.0 or less. However, this new low-cost PEG-hematin can efficiently be used at a very low pH 1.0, and thus it is possible to obtain highly conducting doped PANI (as synthesized) without a need of template.

**$^{15}\text{N}$  NMR Measurement.** The solid-state  $^{15}\text{N}$  CP/MAS NMR spectra of the doped (as synthesized) conducting form of PANI-H, PANI-PVP, and PANI-SPS complex are shown in parts a–c of Figure 4, respectively. The  $^{15}\text{N}$  CP/MAS NMR spectrum of PANI-H shows two resolved resonances in the upfield region of the spectrum. Resonances due to the main-chain amine nitrogen ( $-\text{NH}-$ ) appears at 90.0 ppm while end-group nitrogen ( $-\text{NH}_2$ ) appears at 32.1 ppm. Protonated imine nitrogens ( $=\text{NH}^+-$ ) appear as a broad hump between 100 and 170.0 ppm with broad maximum at  $\sim 109.0$  and  $\sim 142.0$  ppm due to localized charges on the protonated imine nitrogen atom. The strong resonance peak in the  $^{15}\text{N}$  NMR spectrum appears at 90.0 ppm, indicating the delocalization of charges on the nitrogen, i.e., the presence of partially charged nitrogen species. A noticeable exception compared to chemical synthesis is the resonance peak due to the end-group amine nitrogen. This indicates that the enzymatic polymerization yields comparatively lower molecular weight PANI-H. The end-group amine nitrogen is not protonated in this PANI-H. The overall spectral feature of doped PANI-H (as synthesized) is unique and validates the proposed mechanism of charge transport by the “nitrogenonium ion”, in which most of the positive charges reside on the nitrogen atom and very little delocalized into the

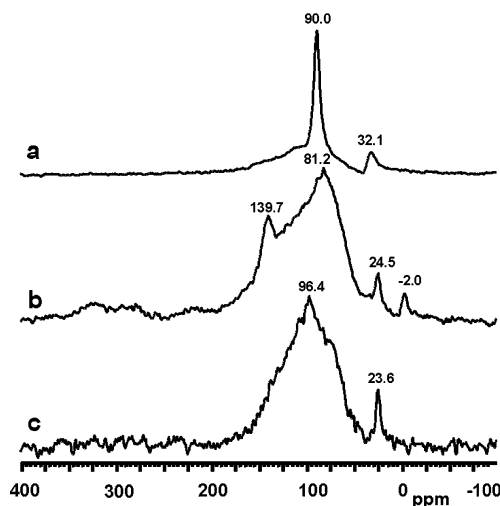


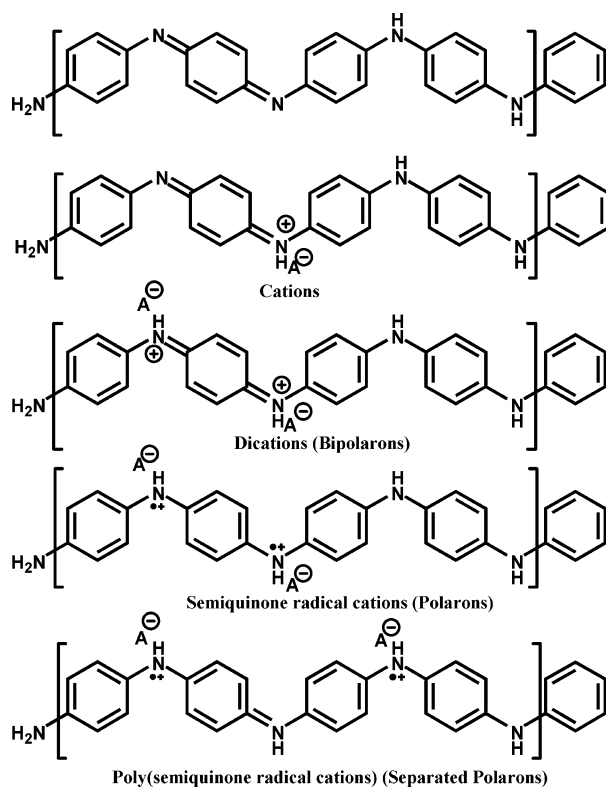
**Figure 4.**  $^{15}\text{N}$  CP/MAS NMR spectra of enzymatically synthesized PANI in its conducting (as synthesized) form: (a) PANI-H; (b) PANI-PVP complex; (c) PANI-SPS complex.

neighboring aromatic rings.<sup>3</sup> However, the hump in the 30.0–100.0 ppm region indicates the broad distribution of charges for amine nitrogen species due to the partially and fully charged imine nitrogen on the neighboring repeating units. The resonance due to imine nitrogens ( $\sim 320.0$  ppm) is not present in the  $^{15}\text{N}$  NMR spectrum, indicating complete protonation during the polymerization and thus providing relatively higher conductivity to this sample.

In contrast,  $^{15}\text{N}$  CP/MAS NMR spectra (Figure 4b,c) of the doped (as synthesized) conducting form of PANI-PVP and PANI-SPS complex show a broad distribution of resonances in the 40.0–200.0 ppm range. These upfield resonances are broad compared to the resonances in the spectrum of Figure 4a. In these samples, the end-group amine nitrogen is protonated (i.e.,  $-\text{NH}_3^+$ ) and appears at 23.6 ppm. In the PANI-PVP complex, the strong peak appears at 81.2 ppm due to delocalization of charges on the nitrogen while fully charged nitrogen species (i.e., nitrogen having a positive charge on it) due to the protonated imine shows a strong peak at 139.7 ppm. In this sample,  $^{15}\text{N}$  resonances from residual uncharged imine nitrogens appear near 300.0 ppm as a broad hump. The partially charged nitrogen resonance for the PANI-SPS complex appears at 96.4 ppm. The broad resonance in the  $^{15}\text{N}$  CP/MAS NMR spectrum for the PANI-SPS complex indicates the presence of PANI, which is not observed in the  $^{13}\text{C}$  CP/MAS NMR spectrum due to overlapping of PANI's resonances with the resonances of the macromolecular template (Figure 1c). The observation of PANI-H without any macromolecular template yields a relatively narrow  $^{15}\text{N}$  resonance in Figure 4a that may be due to the size of the dopant, which is small (i.e., chloride ion), as well as less influence from contribution of the superposition of various structures in Scheme 2.<sup>25</sup> However, in PANI-PVP and PANI-SPS complexes, there may be a broad distribution of nitrogen anion (anion is either bulky phosphate or sulfate groups of the repeating units of the polymer template) interaction resulting from variation of distances due to polymeric nature of anions, leading to a broad distribution of chemical shifts.

Parts a and b of Figure 5 show the  $^{15}\text{N}$  CP/MAS NMR spectra of the dedoped base form of PANI-H and PANI-P, respectively. The  $^{15}\text{N}$  CP/MAS NMR spectrum

### Scheme 2. Different Doped Forms of Conducting PANI



of PANI-H shows two sets of resonances at ca. 50.0–100.0 ppm due to amine nitrogens attached benzenoid rings, whereas imine nitrogens attached to quinoid rings appear at ~320.0 ppm. The integrated area estimated from  $^{15}\text{N}$  resonances for dedoped PANI-H is 5.0 times higher than the doped (as synthesized) sample. This indicates that the most of the resonances are not observed in the doped (as synthesized) PANI-H due to the presence of paramagnetic centers (neighboring polaron lattice). The strong resonance peak at 87.5 ppm is due to residual charged domains in the dedoped base form as discussed earlier and supports the  $^{13}\text{C}$  NMR spectral features in Figure 2 (the shoulder peak at ~128.0 ppm). The resonance peak at 33.0 ppm due to end-group nitrogens appears at the same chemical shift as in the doped sample, suggesting that end groups are not protonated in the doped form. The amine nitrogen peak appears at 68.8 ppm and is nearly 22.0 ppm upfield shift compared to the chemical shifts of doped PANI-H (90.0 ppm, Figure 4a), suggesting that the removal of charge during the dedoping process reflects the large upfield shift of amine resonance and provides evidence for the localization of charges on the nitrogen atom.<sup>30</sup> Deprotonation of charged imine nitrogens also resulted in the ~200.0 ppm downfield shift of imine resonances compared to that of doped form and appear at 326.0 ppm. There is a distinct shoulder at ~302.0 ppm in the imine nitrogen region in Figure 5a, suggesting the coexistence of two types of imine species. However, there is only one resonance for the amine-type nitrogen attached to the benzenoid ring, showing a unique environment for the  $-\text{NH}-$  species as described by Richter et al.<sup>24</sup> This indicates that the PANI-H might contain more oxidized units in the repeating units than reduced units.

Figure 5b shows the  $^{15}\text{N}$  CP/MAS NMR spectrum of the dedoped base form of PANI-P. The upfield reso-

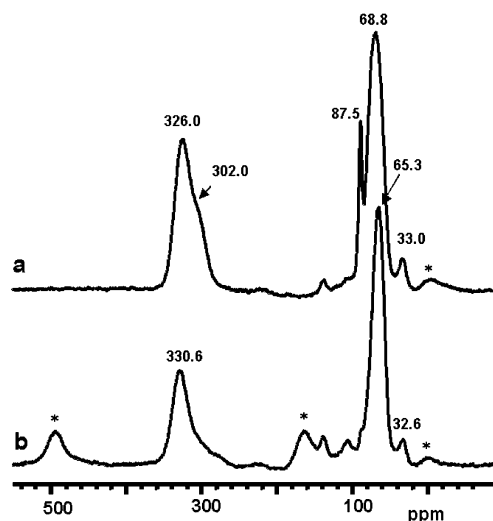


**Figure 5.**  $^{15}\text{N}$  CP/MAS NMR spectra of enzymatically synthesized polyaniline in its dedoped base form: (a) PANI-H; (b) PANI-P (\* denotes spinning sideband).

nance due to the backbone amine nitrogen appears as a narrower peak at 65.3 ppm. As expected, the end-group amine resonances after deprotonation shifts to downfield from 24.5 ppm (Figure 4b) to 32.6 ppm (Figure 5b) and appears at the same place as in Figure 5a. The imine nitrogen, however, shows one resonance peak at 330.6 ppm, and its intensity is relatively small compared to the spectrum in Figure 5a. The 302.0 ppm resonance is not observed in this spectrum, indicating the presence of uniform environments for imine nitrogen in the repeating units. The  $^{15}\text{N}$  spectral feature showing only kind of amine and imine nitrogen species in the repeating units suggests that the fraction of reduced and oxidized units are nearly same; i.e., the structure is similar to the emeraldine base form of PANI.

Figure 6a,b shows  $^{15}\text{N}$  CP/MAS NMR spectra of the redoped form of PANI-H and PANI-P. Although, the redoped PANI shows similar conductivity and  $^{13}\text{C}$  NMR spectral pattern similar to doped (as synthesized) form,  $^{15}\text{N}$  spectral features are quite unusual. After redoping the PANI sample by exposing to hydrochloric acid at pH 1.0, the PANI-H shows a broad distribution of resonances from 0.0 to 250.0 ppm with a maximum at 95.0 ppm. There is an upfield shoulder peak at 70.0 ppm due to uncharged nitrogen species and a downfield shoulder peak at 139.7 ppm due to fully charged nitrogen species. The disappearance of imine nitrogen species (at 330.0 ppm, Figure 5a) indicates complete protonation during redoping (Figure 6a). However, the end-group amine resonance is still without protonation and appears at 32.5 ppm. The redoped form of the PANI-PVP complex shows a similar broad spectral pattern with a variation in the respective chemical shifts and peak intensities. This can be explained by considering the fraction of reduced and oxidized units in both samples. In contrast, in redoped PANI-P, the 65.0 ppm peak due to uncharged nitrogen species of the reduced unit is dominant. The spectral broadening upon doping with mineral acid may be due to the superposition of various structures in Scheme 2 (excluding structures containing cation radicals) and their distribution. This may indicate that the difference in chemical shifts between doped and dedoped PANI forms originating from partial charges on nitrogen leads to a variation in the chemical shifts of resonances associated with ben-

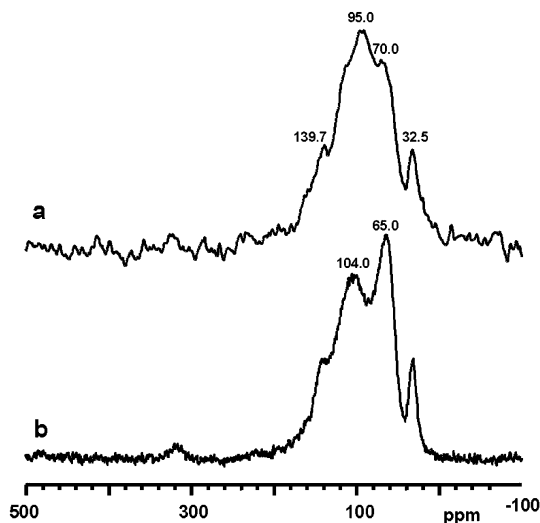


**Figure 6.**  $^{15}\text{N}$  CP/MAS NMR spectra of enzymatically synthesized polyaniline in its redoped conducting form: (a) PANI-H; (b) PANI-P (redoping was carried out in HCl medium).

zenoid species. In the case of  $^{13}\text{C}$  CP/MAS NMR as the charge center is not on the ring carbons, the shift is marginal ( $\sim 5.0$  ppm) whereas in the case of  $^{15}\text{N}$  CP/MAS NMR, depending on the extent of delocalization it varies in the range 15.0–25.0 ppm due to nitrogen charge carrier in the polyaniline. This observation to our knowledge is unique to enzymatically prepared PANI polymer, suggesting contributions from the bipolaronic conduction mechanism.

**Redoping at Different pH.** Polyaniline shows doping/dedoping reversibility, since it is possible to dedope and redope the polymer by varying the pH of the solution. In enzymatically polymerized PANI-SPS and PANI-PVP complex reversible doping/dedoping behavior shows hysteresis as a function of pH, though the latter also shows time-dependent changes in the polaron band region of UV-vis-near-IR spectra.<sup>9,11</sup> To study this behavior by NMR, the pH value of the dedoped base form of PANI-P is decreased from 7 to 1 by the addition of the appropriate amount of 1 N HCl solution to a suspension of the dedoped complex in water. Figures 7 and 8 shows  $^{13}\text{C}$  and  $^{15}\text{N}$  CP/MAS NMR spectra obtained at different pH during the redoping of the dedoped base form of PANI-P to study the changes in the spectral pattern in the insulator-metal transition regime. At pH 7.0, the  $^{13}\text{C}$  and  $^{15}\text{N}$  CP/MAS NMR spectra resemble well with the base form spectrum. Comparing the  $^{13}\text{C}$  CP/MAS NMR spectral features in Figures 7a and 2b, only difference is the intensity of the 128.5 ppm shoulder which is due to the presence of some charges on the neighboring nitrogen atom attached to aromatic ring carbons. After decreasing the pH to 5.0, the  $^{13}\text{C}$  and  $^{15}\text{N}$  CP/MAS NMR spectra shows broad changes pertaining to the reduction of imine nitrogen species, which gets protonated. This is reflected in the reduction of peak at 137.0 and 157.0 ppm in the  $^{13}\text{C}$  CP/MAS NMR spectrum (Figure 7b) and 330.0 ppm resonance in the  $^{15}\text{N}$  CP/MAS NMR spectrum (Figure 8b). At the expense of these resonances the resonance intensity of 128.6 ppm in  $^{13}\text{C}$  and 106.1 ppm resonance in  $^{15}\text{N}$  NMR spectra increases. There is a dramatic change in  $^{13}\text{C}$  and  $^{15}\text{N}$  CP/MAS NMR spectra obtained after decreasing the pH to 3.0. In Figure 7c, the reduction in carbons from quinoid rings decreases, and now the peak maximum shifts to 128.5 ppm rather than

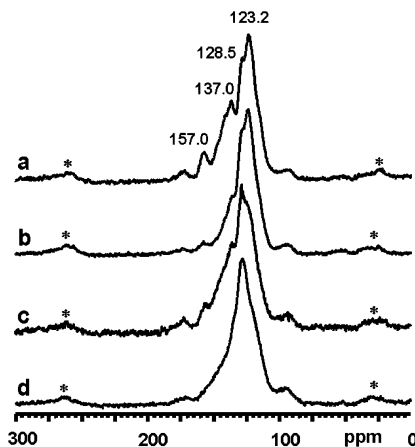


**Figure 7.**  $^{13}\text{C}$  CP/MAS NMR spectra of PANI-P at different pH during the redoping process from the dedoped base form: (a) pH 7.0; (b) pH 5.0; (c) pH 3.0; (d) pH 1.0 (\* denotes spinning sideband).

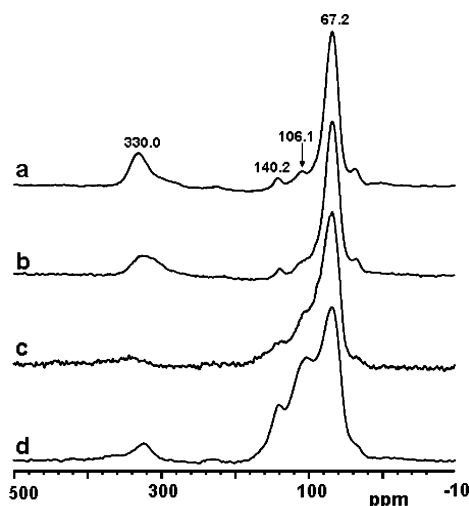


**Figure 8.**  $^{15}\text{N}$  CP/MAS NMR spectra of PANI-P at different pH during the redoping process from the dedoped base form: (a) pH 7.0; (b) pH 5.0; (c) pH 3.0; (d) pH 1.0.

123.2 ppm. Similarly the  $^{15}\text{N}$  CP/MAS NMR spectrum in Figure 8c shows complete disappearance of the imine nitrogen peak at 330.0 ppm, and the higher intensity of the downfield tail of the amine peak at 67.2 ppm resembles that of the chemically synthesized PANI spectrum reported by Espe et al.<sup>21</sup> Interestingly, the resonance at 33.0 ppm due to end-group  $-\text{NH}_2$  species shows no change in the intensity and partially buried under the broad distribution of amine and protonated imine resonance. The resonance intensity of partially and fully charged protonated imine nitrogen species at 106.1 and 140.2 ppm increases, and spectrum is noisy as the contribution from polaronic lattice interaction increases, resulting in the disappearance of those species which are near the polarons, i.e., radical cations. The decrease in signal-to-noise ratio is also observed in Figure 8c. Further decrease of solution pH to 1.0 resulted in the disappearance of carbon resonances from quinoid rings (Figure 7d). The spectral feature resembles with the redoped form of PANI-P (Figure 3b) and the resonance at 128.6 ppm, which can be due to the bipolaronic state of the polyaniline repeating units. The shift in resonance position in the  $^{13}\text{C}$  NMR spectrum in the doped-dedoped cycle is clearly evident. The  $^{15}\text{N}$  CP/MAS NMR spectrum also resembles the redoped

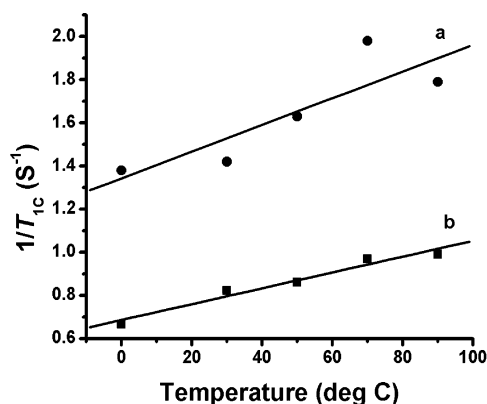


**Figure 9.**  $^{13}\text{C}$  spin-lattice relaxation rates ( $1/T_{1C}$ ) vs temperature of PANI in doped (as synthesized) conducting form: (a) PANI-H; (b) PANI-PVP complex.

PANI-P (Figure 6b). The peak corresponding to partially and fully charged nitrogen species is distinct and spreads up to the 200.0 ppm region. There are residual imine nitrogens still present, suggesting that there are some domains that are unable to protonate even at lower pH value. The amine resonances appear at 66.0 ppm. However, the signal-to-noise ratio in  $^{13}\text{C}$  and  $^{15}\text{N}$  CP/MAS NMR spectra obtained after redoping at pH 1.0 is higher than that of pH 3.0, suggesting that as the degree of protonation or doping increases, the fraction of polaronic lattice increases, and then after reaching maximum value, the concentration of polarons starts decreasing, at which bipolarons become predominant charge carriers. This trend is evident from ESR studies carried out by Epstein et al.<sup>31</sup> with doping level as the free radical concentration increases with increasing doping level in the beginning, and at the higher level doping, free radical concentration decreases. Similarly, since NMR is invisible to polarons lattice and those near its center, the increase in polaronic contribution resulted in decrease of signal-to-noise ratio, but as bipolaronic state starts dominating, the signal-to-noise ratio, i.e., fraction of total carbon or nitrogen atom observed, increases.

**Variable Temperature Solid-State NMR.** Variable temperature relaxation measurements were made to further substantiate the contributions from the conduction electrons. Figure 9 shows the  $^{13}\text{C}$  spin-lattice relaxation rates ( $1/T_{1C}$ ) as a function of temperature in PANI-H and PANI-PVP complexes. The  $T_1$  measurements were made at five different temperatures between 0 and 90 °C. A point to note that there is no change in the line shape during the variable temperature measurements. The polyaniline prepared from PEG-hematin-catalyzed polymerization at lower pH 1.0, which shows higher conductivity and also shows lower  $T_{1C}$  compared to that of doped PANI-PVP complex. A linear dependence of  $1/T_{1C}$  with temperature is observed, suggesting the role of Korringa-type relation for the spin-lattice relaxation mechanism in classical metals.<sup>29</sup>

**Molecular Weight Determination.** The molecular weight of enzymatically synthesized PANI was determined by the end-group analysis technique according to Adams et al.<sup>32</sup> This method allows to estimate the number of repeating units in average PANI backbone by measuring the ratio of the integrated areas of secondary to primary amine groups from the well-resolved  $^{15}\text{N}$  CP/MAS NMR spectrum. It is assumed

**Table 1. Integrated Peak Areas Determined from  $^{15}\text{N}$  CP/MAS NMR of the Dedoped Base Form of Enzymatically Synthesized PANI**

	cross-polarization contact time (ms)	ratio of peak areas in $^{15}\text{N}$ CP/MAS NMR spectrum			av mol wt (no. of repeating units)
		imine	secondary amine	primary amine	
PANI-H	0.5	2.42	22.36	1	4072 (45)
	1.0	3.78	23.20	1	
	2.0	7.84	22.28	1	
	5.0	17.21	22.13	1	
PANI-P	0.5	3.91	11.83	1	2715 (28)
	1.0	7.11	12.63	1	
	2.0	10.60	15.88	1	
	5.0	14.51	15.45	1	

that the polymer chains have one  $-\text{NH}_2$  end group and appear at ca. 32 ppm in the  $^{15}\text{N}$  NMR spectrum of enzymatically synthesized PANI. However, the cross-polarization is a dynamic process, and the intensity obtained is not only depends on the nature of nitrogen species but also on its chemical environment (i.e., the number of attached hydrogen). However, variable contact time experimental data on the dedoped (base) form of PANI indicate that the intensity variation in both secondary and primary amine resonance follows a similar trend of major resonance peaks in the  $^{15}\text{N}$  NMR spectrum and can be reasonably quantified to compare their molecular weights of enzymatically synthesized PANI. The integrated areas for imine and secondary amine nitrogens at different contact times in  $^{15}\text{N}$  CP/MAS NMR experiment were obtained by normalizing the area of primary amine resonance peak to 1 and are presented in Table 1. The average ratio of secondary to primary amine nitrogens in the dedoped (base) form of the PANI-H is 22.5:1, indicating an average number of repeating units is 45. The ratio of secondary to primary amine remains almost constant with contact time indicates the validity of calculation. The dedoped form of PANI-P shows that the average ratio of secondary to primary amine nitrogens is 14:1, suggesting an average number of repeat units for this polymer are 28. The estimated molecular weights obtained for two polyaniline are 4072 for PANI-H whereas 2715 for PANI-P. This is consistent with the results that the chain lengths play a crucial role in the conduction mechanism; the PANI with a high molecular weight exhibits higher conductivity.

## Conclusions

Solid-state  $^{13}\text{C}$  and  $^{15}\text{N}$  CP/MAS NMR studies of the various forms of PANI prepared by enzymatic polymerization using HRP and PEG-hematin as catalysts showed broad variation in their chemical and electronic structures. The spectral features obtained from  $^{13}\text{C}$  and  $^{15}\text{N}$  CP/MAS NMR spectra of PANI in three different forms (doped (as synthesized) conducting, dedoped base, redoped conducting) show that the PANI-H shows more resemblance to chemically synthesized PANI, whereas PANI-P shows features that are unique to the enzymatically synthesized polymer.  $^{15}\text{N}$  CP/MAS NMR of the dedoped PANI sample indicates that PANI-H may be overoxidized, whereas PANI-P shows 1:1 imine-to-amine nitrogens. However, the redoped PANI-H shows entirely different features than the doped (as synthesized) form and indicates that although the redoping process can retrieve the conductivity, the charge distribution along the PANI backbone is more inhomogeneous compared to the doped (as synthesized) form. The

sequential redoping of HRP-catalyzed dedoped PANI—P shows transformation of amine to imine and charge delocalization effect on the spectral features. The charge carriers during conduction are believed to be both bipolarons having dicationic lattice and polarons having semiquinone radical structures. It was established during this study that the  $^{13}\text{C}$  line width is greatly influenced by the conductivity, and the higher conducting sample shows a broader line width. The presence of the bipolaronic state in the doped state resulted in the shift of the  $^{13}\text{C}$  NMR resonance to ca. 5.0 ppm downfield compared to the dedoped form, whereas the  $^{15}\text{N}$  NMR resonance almost shifted downfield by 20.0–25.0 ppm. Another interesting observation is that the S:N ratio in  $^{13}\text{C}$  and  $^{15}\text{N}$  CP/MAS NMR shows the increase influence of polaronic contribution to the PANI structure (lowest S:N ratio) around pH 3.0, but at lower pH, the bipolaronic contribution becomes dominant.

**Acknowledgment.** The authors thank the National Science Foundation for the research grant (Grant DMR-9986644) and Drs. Wei Liu and Ferdinando Bruno for helpful discussions.

## References and Notes

- (1) MacDiarmid, A. G. *Angew. Chem., Int. Ed.* **2001**, *40*, 2581.
- (2) MacDiarmid, A. G. *Synth. Met.* **1997**, *84*, 27.
- (3) MacDiarmid, A. G.; Chiang, J. C.; Richter, A. F.; Epstein, A. J. *Synth. Met.* **1987**, *17*, 285.
- (4) MacDiarmid, A. G.; Epstein, A. J. *Faraday Discuss. Chem. Soc.* **1989**, *88*, 317.
- (5) Prigodin, V. N.; Epstein, A. J. *Synth. Met.* **2002**, *125*, 43.
- (6) Epstein, A. J.; MacDiarmid, A. G. *Synth. Met.* **1991**, *41–43*, 601.
- (7) Pouget, J. P.; Laridjani, M.; Jozefowicz, M. E.; Epstein, A. J.; Scherr, E. M.; MacDiarmid, A. G. *Synth. Met.* **1992**, *51*, 95.
- (8) Samuelson, L. A.; Anagnostopoulos, A.; Alva, K. S.; Kumar, J.; Tripathy, S. K. *Macromolecules* **1998**, *31*, 4376.
- (9) Liu, W.; Kumar, J.; Tripathy, S.; Senecal, K. J.; Samuelson, L. A. *J. Am. Chem. Soc.* **1999**, *121*, 71.
- (10) Liu, W.; Cholli, A. L.; Nagarajan, R.; Kumar, J.; Tripathy, S.; Bruno, F. F.; Samuelson, L. A. *J. Am. Chem. Soc.* **1999**, *121*, 11345.
- (11) Nagarajan, R.; Tripathy, S.; Kumar, J.; Bruno, F. F.; Samuelson, L. A. *Macromolecules* **2000**, *33*, 9542.
- (12) (a) Sahoo, S. K.; Nagarajan, R.; Samuelson, L. A.; Kumar, J.; Cholli, A. L.; Tripathy, S. K. *J. Macromol. Sci., Pure Appl. Chem.* **2001**, *A38*, 1315. (b) Sahoo, S. K.; Nagarajan, R.; Roy, S.; Samuelson, L. A.; Kumar, J.; Cholli, A. L. *Polym. Mater. Sci. Eng.* **2002**, *87*, 394.
- (13) Liu, W.; Kumar, J.; Tripathy, S. K.; Samuelson, L. A. *Langmuir* **2002**, *18*, 9696.
- (14) Sahoo, S. K.; Nagarajan, R.; Chakraborty, S.; Samuelson, L. A.; Kumar, J.; Cholli, A. L. *J. Macromol. Sci., Pure Appl. Chem.* **2002**, *39*, 1223.
- (15) Roy, S.; Fortier, J. M.; Nagarajan, R.; Tripathy, S. K.; Kumar, J.; Samuelson, L.; Bruno, F. F. *Biomacromolecules* **2002**, *3*, 937.
- (16) Bruno, F. F.; Nagarajan, R.; Roy, S.; Kumar, J.; Tripathy, S.; Samuelson, L. A. *Mater. Res. Soc. Symp. Proc.* **2001**, *660*, J18.6/1.
- (17) Roy, S.; Nagarajan, R.; Sahoo, S. K.; Bruno, F. F.; Tripathy, S. K.; Kumar, J.; Samuelson, L. A. Private communication.
- (18) Hjertberg, T.; Salaneck, W. R.; Lundstrom, I.; Somasiri, N. L. D.; MacDiarmid, A. G. *J. Polym. Sci., Polym. Lett.* **1985**, *23*, 503.
- (19) Kaplan, S.; Conwell, E. M.; Richter, A. F.; MacDiarmid, A. G. *J. Am. Chem. Soc.* **1988**, *110*, 7647.
- (20) Stein, P. C.; Hartzell, C. J.; Jorgensen, B. S.; Earl, W. L. *Synth. Met.* **1989**, *29*, E297.
- (21) Espe, M. P.; Mattes, B. R.; Schaefer, J. *Macromolecules* **1997**, *30*, 6307.
- (22) Kababya, S.; Appel, M.; Haba, Y.; Titelman, G. I.; Schmidt, A. *Macromolecules* **1999**, *32*, 5337.
- (23) Kaplan, S.; Conwell, E. M.; Richter, A. F.; MacDiarmid, A. G. *Synth. Met.* **1989**, *29*, E235.
- (24) Richter, A. F.; Ray, A.; Ramanathan, K. V.; Manohar, S. K.; Furst, G. T.; Opella, S. J.; MacDiarmid, A. G. *Synth. Met.* **1989**, *29*, E243.
- (25) Wehrle, B.; Limbach, H.-H.; Morteensen, J.; Heinze, J. *Angew. Chem., Int. Engl. Adv. Mater.* **1989**, *28*, 1741.
- (26) Kenwright, A. M.; Feast, W. J.; Adams, P.; Milton, A. J.; Monkman, A. P.; Say, B. J. *Synth. Met.* **1993**, *55–57*, 666.
- (27) Young, T. L.; Espe, M. P.; Yang, D.; Mattes, B. R. *Macromolecules* **2002**, *35*, 5565.
- (28) Mathew, R.; Yang, D.; Mattes, B. R.; Espe, M. P. *Macromolecules* **2002**, *35*, 7575.
- (29) Kolbert, A. C.; Caldarelli, S.; Their, K. F.; Sariciftci, N. S.; Cao, Y.; Heeger, A. J. *Phys. Rev. B* **1995**, *51*, 1541.
- (30) Chaloner-Gill, B.; Euler, W. B.; Mumbauer, P. D.; Roberts, J. E. *J. Am. Chem. Soc.* **1991**, *113*, 6831.
- (31) Epstein, A. J.; Ginder, J. M.; Zuo, F.; Woo, H. S.; Tanner, D. B.; Richter, A. F.; Angelopoulos, M.; Huang, W. S.; MacDiarmid, A. G. *Synth. Met.* **1987**, *21*, 63.
- (32) (a) Adams, P. N.; Monkman, A. P.; Apperley, D. C. *Synth. Met.* **1993**, *55–57*, 725. (b) Adams, P. N.; Apperley, D. C.; Monkman, A. P. *Polymer* **1993**, *34*, 328.

MA035252+